

Soft Matter

Accepted Manuscript



This is an *Accepted Manuscript*, which has been through the Royal Society of Chemistry peer review process and has been accepted for publication.

Accepted Manuscripts are published online shortly after acceptance, before technical editing, formatting and proof reading. Using this free service, authors can make their results available to the community, in citable form, before we publish the edited article. We will replace this *Accepted Manuscript* with the edited and formatted *Advance Article* as soon as it is available.

You can find more information about *Accepted Manuscripts* in the [Information for Authors](#).

Please note that technical editing may introduce minor changes to the text and/or graphics, which may alter content. The journal's standard [Terms & Conditions](#) and the [Ethical guidelines](#) still apply. In no event shall the Royal Society of Chemistry be held responsible for any errors or omissions in this *Accepted Manuscript* or any consequences arising from the use of any information it contains.

Cite this: DOI: 10.1039/c0xx00000x

www.rsc.org/xxxxxx

ARTICLE TYPE**Photo-responsive Superhydrophobic Coating for Regulating Boundary Slippage**Yang Wu,^{ab} Zhilu Liu,^a Yongmin Liang,^a Xiaowei Pei^a, Feng Zhou^{a*} and Queji Xue^a*Received (in XXX, XXX) Xth XXXXXXXXX 20XX, Accepted Xth XXXXXXXXX 20XX*

DOI: 10.1039/b000000x

A photoresponsive copolymer containing catechol and azobenzene derivatives was synthesized. The copolymer easily attached onto various substrates and showed a photoresponsive characteristic because of its catechol and azobenzene functional groups. The copolymer was successfully assembled on nanoparticles, plate mica, and rough anodized aluminum surface. The rough anodized aluminum sheet retained a Cassie–Baxter state after being modified with the copolymer. Moreover, surface adhesion can be interchanged by changing the UV exposure time. The sliding and adhesive states of water droplets were achieved by UV exposure and dark storage. Boundary slip on the rough sheet was measured using a commercial rheometer, and interchangeable slip length was also obtained after irradiation or storage. The versatile, substrate-independent approach may be significant in the development of new materials for smart fluid devices.

Cite this: DOI: 10.1039/coxx00000x

www.rsc.org/xxxxxx

ARTICLE TYPE

Introduction

Based on the difference among surface adhesion forces on superhydrophobic surfaces, two superhydrophobic wetting states can be obtained, namely, Cassie–Baxter state (superhydrophobic and with low adhesion force) and Wenzel state (superhydrophobic and with high adhesion force). Both these special wetting states were copied from plants^{1, 2}. Recently, superhydrophobic surfaces, especially the responsive surfaces, have become one of the top research subjects because of their special wetting properties^{3, 4}, and potential applications^{5, 6}. Many responsive surfaces have already been prepared, and their wetting states or surface adhesion forces are regulated by the external environment such as temperature⁷, irradiation⁸, solvent⁹, or electromagnetic field^{10, 11}. In recent studies, our group constructed a series of responsive superhydrophobic surfaces on anodized alumina¹² by grafting a responsive polymer brush, and obtained the interchangeable surface adhesion force by altering the ambient temperature and pH of the water droplet. TiO₂ nanotube surface shows Cassie state after silanization, but shows Wenzel state with high adhesion after selective UV exposure through a mask¹³. In 2007, Lee¹⁴ discovered the mechanism of dopamine (DOPA) as the universal anchor group from a mussel. The bioinspired catecholic chemistry for surface modification has been attracting attention from researchers¹⁵. Many functions of small DOPA molecules or DOPA polymers have been studied for one-step functionalization¹⁶, such as atom transfer radical polymerization (ATRP) initiator¹⁷, scaffold materials of stem cell¹⁸, antifouling¹⁹, surface wetting states^{20, 21}, and so on. The catechol group was used as a universal layer-by-layer (LBL) primer because it can adsorb onto almost all surfaces²².

In regard to these responsive surfaces, most studies placed emphasis on the static wetting characteristics, including the contact angle, sliding angle, and surface adhesion. The behaviors of the dynamic flow of these responsive surfaces are rarely reported, especially the fluid boundary slip of the responsive superhydrophobic surface. When a fluid flows on a solid surface, a drag always exists between the liquid and solid surface, which can result to a series of problems that includes increasing energy consumption, heating of devices, and surface wear and tear. The existence of air bubbles between the liquid and superhydrophobic surfaces produces an air layer that supports fluids above the solid surface, and the “fluid-solid” shears are replaced by “fluid-air” shears. Thus, the drag-reducing characteristic appears. In previous studies involving the drag reduction of superhydrophobic surface, researchers focused on the microcosmic morphology of the said surface, which influences the boundary slip. Truesdell²³ studied two surfaces, one of which has a regular groove with a superhydrophobic coating, while the other has a smooth surface and found that longitudinal grooves are necessary to produce large slip lengths. Lee²⁴ achieved a maximum slip length of 400 μm on dual-scale structures (micro-nano), which is larger than the maximum 180 μm slip length reported on the single-scale (micro-smooth) structures. “Posts” and “grates” surfaces with varying gas fractions were also constructed by his group²⁵, and they found that in the samples with the same target gas fraction, the slip length of the “grates” surface was larger than the “posts” surface.

Recently, we focused on the effects of surface adhesion on the boundary slippage²⁶. A series of adhesion-regulated superhydrophobic surfaces were prepared, and the study revealed that the boundary slippage decays with increasing surface adhesion, and an interchangeable boundary slippage can be obtained by altering the testing temperature. In this present work, we synthesized a type of photoresponsive monomer, and then copolymerized it with the adhesive DOPA group. The two groups endowed the polymer with photoresponsiveness and a favorable film-forming characteristic. The copolymer was assembled on three substrates to prove the excellent film-forming characteristic. Moreover, after the assembly on a rough anodized aluminum sheet, the surface showed a superhydrophobic state with low adhesion, (sliding angle < 5°). After a certain time under UV exposure, the surface adhesion changed. The water droplet adhered onto the surface with a superhydrophobic state. Then, the adhesive state can be changed into sliding state after dark storage. The different wetting states of the surface influenced the fluid slip and were detected using a rheometer. The slip length of the reversible fluid was interchanged by the UV exposure and dark storage. This responsive surface can be applied to intelligent microfluidics devices to regulate flow.

Experiment

Materials

4-(Trifluoromethoxy)aniline(99%, J&K Chemical Corp.) 2, 2-azobisisobutyronitrile (AIBN, Aldrich) was re-crystallized from ethanol. 3-Hydroxytyramine hydrochloride (dopamine-HCl, Aldrich), methacryloyl chloride (Alfa Aesar), Na₂B₄O₇·10H₂O, Na₂CO₃·H₂O (Tianjin Chemical Reagents Corp., China) and phenol(Sinopharm, China) was used as received.

Monomer synthesis

4-Hydroxy-4'-trifluoromethoxy-azobenzene (HOFAZO) was synthesized according to previous literature²⁷. Golden crystals were obtained after recrystallization in n-hexane. 2.81 g the golden solid(HOFAZO) and 2 ml triethylamine dissolved in 50 ml dried dichloromethane at 0 °C. Then a dichloromethane solution with 1.5 ml methacryloyl chloride dropwise added to above solution. The reaction mixture was stirred at 0 °C for 5 h under Ar. The reaction solution was wash with saturated NaCl solution. The combined organic extracts were dried over anhydrous MgSO₄, and the solvent was evaporated under reduced pressure to give a deep yellow solid. The crude product was purified by silica gel column chromatography to give a yellow solid. ¹H NMR (400 MHz, Chloroform-d, ppm): δ: 7.99-7.89 (m, 4H), 7.37-7.25 (m, 4H), 6.37 (t, 1H), 5.79 (t, 1H), 2.07 (m, 3H). N-(3,4-dihydroxyphenyl)ethyl methacryl amide (DOPAMA)was synthesized according to our reported²⁸.

Polymerization

FAZO monomer (0.36 g, 1 mmol), DOPAMA (22 mg, 0.1 mmol), and AIBN (6.0mg, 0.036 mmol) were dissolved in 3 mL dimethyl formamide (DMF). The solution was heated to 70 °C and kept for 24 h after degassing with Ar for 15 min. The polymers(FAZO-DOPA) obtained were precipitated by ethanol,

and purified by repeated washings with ethanol. The purified polymers were dried under reduced pressure at 40 °C for 24 h.

FTIR (KBr, cm⁻¹): 3460 (phenolic hydroxyl), 3070 (stretching, C-H of benzene ring), 2946, 2988 (stretching, CH₂ and CH₃), 1755 (stretching, -C=O).

Film formation

The typical procedure of film formation on solid surface is as following: Polymer solution was prepared by dissolving FAZO-DOPA in acetone at a concentration of 2 wt.%. The freshly TiO₂ nano particles was dispersed in the solution at room temperature for 48 h and then rinsed thoroughly with acetone. Finally, the treatment of the modified TiO₂ nano particles dried at 40 °C under vacuum condition. Preparation of the self-assembly polymer films was carried out on the surface of anodised aluminium, mica and titanium by the same method.

Characterizations

¹H NMR spectra were recorded on a Varian Unity Inova 400 FT-NMR spectrometer operated at 400 MHz. Infrared spectroscopic measurements were conducted on a TENSOR 27 instrument (KBr, disk). The UV-Vis absorption spectra were recorded on a Specord 50 spectrophotometer (Analytik Jena, Germany) at 1 cm path length. Chemical element composition information about the samples was obtained by X-ray photoelectron spectroscopy (XPS), the measurement was carried out on a PHI-5702 multifunctional spectrometer using Al K α radiation, and the binding energies were referenced to the C1s line at 284.8 eV from adventitious carbon. Surface topography of the self-assembly films on mica was imaged using an atomic force microscope using an atomic force microscope (AFM) (Agilent 5500) in contact tapping mode. Scanning electron microscope (SEM) images were obtained on a JSM-6701F field emission scanning electron microscope (FE-SEM) at 5–10 kV. Sessile water droplet contact angle (CA) values were acquired using a DSA-100 optical contact angle meter (Kruss Company, Ltd, Germany) at ambient temperature (20°C). 5 μ L deionized water was dropped on the samples (anodised aluminium and titanium modified with the copolymer) using an automatic dispense controller, and the contact angles were determined automatically by using the Laplace-Young fitting algorithm. The average CA values were obtained by measuring the sample at different positions on the substrate. The thicknesses of the polymer films on titanium were measured using an ellipsometer (L116E, Gaertner, USA). A 300 W high-pressure mercury lamp was used as the light source for the photo-switch of FAZO-DOPA copolymer. Light was passed through a cut-off filter ($\lambda = 365$ nm for UV) and the intensity of the UV irradiation is 30.8 mW/cm². The morphology of modified particles was investigated on transmission electron microscopy (TEM) (TECNAI G2 TF20 apparatus). Thermal stability was determined with a thermogravimetric analyzer (TGA) (Netzsch, STA 449 C) over a temperature range of 50–700 °C at a heating rate of 10 °C/min under N₂ atmosphere. Boundary slippage was measured on a rheometer (HAAKE, RS6000, Germany). For this experiment, plate-and-plate model was applied: a stainless steel clamp with a diameter (2R) of 35mm, modified substrates as the first plate, and standard smooth stainless plate was considered the non-slip plate. Temperature was controlled with the error less 0.1°C, the distance (H) between the clamp and test surface was measured by rheometer precisely. The fixed volume test liquid (distilled water) was injected into the gap by syringe. The clamp is driven by a given certain angular velocity. If slip exists on a

surface, the clamp will have different shear stress, which is recorded by the controlling computer.

Results and discussion

The copolymer FAZO-DOPA was synthesized by polymerization of FAZO and DOPA monomer in DMF using AIBN as initiator. **Scheme 1** shows the fabrication process of the catechol-containing polymer. The assembly of catecholic compounds onto various substrates has already been proven¹⁴. The copolymer also produced a favorable film-formation characteristic, and the assembled surface possessed photoresponsive characteristic because of its FAZO and DOPA composition. The UV-Vis absorption spectra of the copolymer in acetone are shown in **Fig. 1**. The maximum absorbance was at 330 nm, which is attributed to the π - π^* stacking of *trans*-azobenzene. After UV exposure, the intensity of the π - π^* transition band at 330 nm decreased as a result of *trans-cis* conversion. With increasing UV exposure time, the intensity of maximum absorption peak decreased as the *trans* structure content of FAZO also decreased. Moreover, after 130 min of UV exposure, the maximum absorbance was reduced by more than half, which means more than half of the *trans* structure of FAZO was converted to *cis*. The copolymer assembled onto the TiO₂ nanoparticles, and this was confirmed using FTIR, XPS, TGA, TEM, and through dispersion in ethanol and acetone, as shown in **Fig. 2**. The representative full-scan spectra of the original TiO₂ particles and assembled particles are shown in **Fig. 2a**. After assembling with the copolymer, a strong signal for F_{1s} at 689.0 eV appeared, and the N_{1s} absorption signal emerged at 400.1 eV. However, for the original TiO₂ nanoparticles, the XPS singles of its two characteristic elements did not appear. The TGA curves of TiO₂ nanoparticles, assembled TiO₂ nanoparticles, and the FAZO-DOPA copolymer are shown in **Fig. 2b**. The TiO₂ nanoparticles did not decomposed until the temperature reached 700 °C, but the copolymer began to decompose at about 350 °C. In addition, the weight loss of TiO₂ nanoparticles assembled with FAZO-DOPA was 11.2% and decomposed within the range of 350 °C to 450 °C. The decomposition temperature had no difference with the FAZO-DOPA. The TEM images shown in **Figs. 2c and 2d** are excellent proofs for the assembly of copolymer on the TiO₂ nanoparticles. The high-resolution TEM images clearly show the boundary interface between the unmodified particles and copper mesh basement (**Fig. 2c**). However, for the particles that assembled with the copolymer, a shadowy boundary interface appeared, and the thickness of interface was about 2 nm. These results prove that the copolymer film successfully assembled on TiO₂ nanoparticles. The dispersivity of the two particles was demonstrated in ethanol and acetone after standing for 24 h (**Figs. 2e and 2f**). The unmodified TiO₂ nanoparticles showed good dispersivity in ethanol, and opacity in solution, which is maintained after storing for 24 h. However, the raw TiO₂ showed poor dispersivity in acetone as nanoparticles subsided to the bottom, and the solution became transparent (**Fig. 2e**). The results were different for the modified TiO₂ nanoparticles as they showed poor dispersivity in ethanol but good dispersivity in acetone (**Fig. 2f**). The main reason behind their dispersivity is that the copolymer cannot dissolve in ethanol, but dissolves in acetone. That is the reason why in the preparation, we used ethanol as the precipitant to obtain the copolymer. All the above results proved that the FAZO-DOPA copolymer successfully assembled onto the TiO₂ nanoparticles.

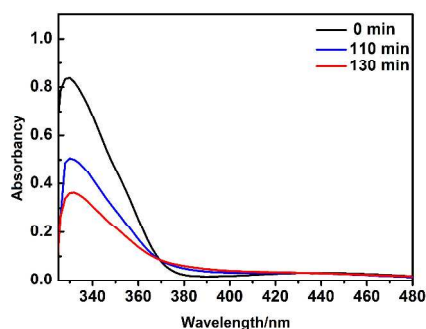
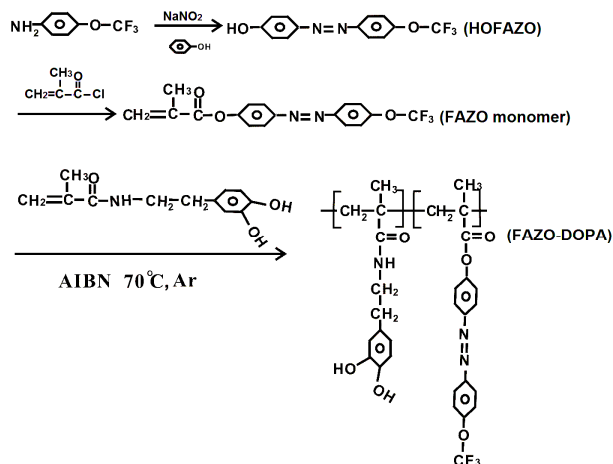


Fig 1. UV-vis absorption spectra of FAZO-DOPA in acetone solution after UV exposure.

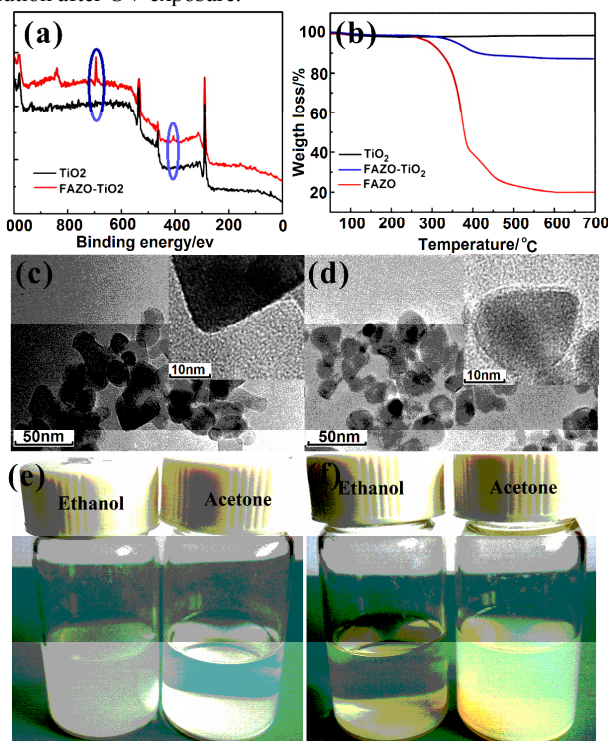


Fig 2. (a) XPS survey spectra and (b) TGA curves of TiO_2 nanoparticles with and without FAZO-DOPA modification; TEM images of (c) raw TiO_2 and (d) modified TiO_2 nanoparticles; dispersion of (e) raw TiO_2 and (f) modified TiO_2 nanoparticles.

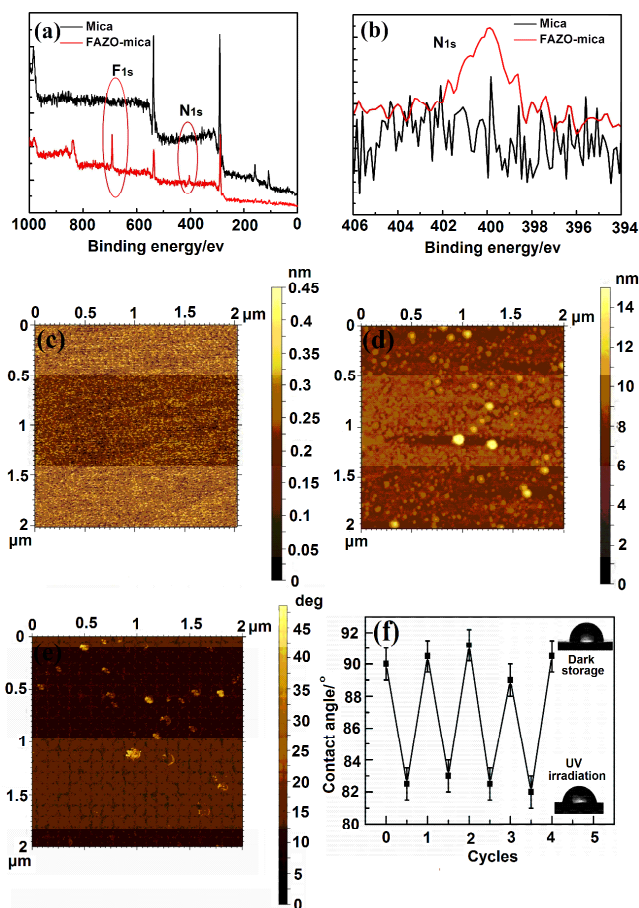


Fig 3. (a) Full XPS spectra and (b) N element fine spectra of modified and non-modified mica; AFM morphology images of (c) unmodified and (d) modified mica. (e) The AFM phase image of modified mica. (f) The reversible wettability of flat Ti surface after exposure with UV and storage in dark.

The catechol-containing polymer assembled on a flat mica surface. The elemental analysis and the morphology of the FAZO-DOPA polymer on mica were investigated using XPS and AFM, respectively. **Fig. 3a** shows the full XPS spectra of the unmodified and modified mica. After the polymer assembled, the characteristic F and N elemental singles appeared. **Fig. 3b** shows the fine spectrum of N, while **Fig. 3c** shows the morphology of the original mica displaying a very smooth surface. After the modification of the FAZO-DOPA polymer, randomly distributed polymer islands appeared, as shown in **Fig. 3d**. **Fig. 3e** shows the AFM phase image of modified mica surface. The results indicate that the area surrounding the polymer aggregations was coated with a polymer layer and that the whole surface was chemically homogeneous. Thus, a dense and homogeneous polymer layer was achieved with a thickness of approximately ~ 6 nm on a flat titanium surface. From the elemental analysis and the morphological analysis of flat mica, we conclude that the copolymer also successfully assembled on the flat mica surface.

The azobenzene molecules containing $-\text{CF}_3$ group have a *trans* conformation with a small dipole moment and a low surface free energy. The $-\text{CF}_3$ groups preferentially accumulate on the top surface, which leads to the hydrophobic characteristics. After UV exposure, the azobenzene molecules acquired a *cis* conformation having a large dipole moment. and a preferential accumulation on the top surface with a slightly higher surface free energy. Some

hydrogen bonds also formed between the FAZO groups and water molecules, which led to a large surface adhesion or wetting state transformation. Lim⁸ fabricated a photo-interchangeable surface using LBL assembling SiO₂ and introduced photosensitive moieties onto the top surface. After UV exposure, the interchangeable wetting state of the surface can now interconvert from the superhydrophobic state to the superhydrophilic state. Liu²⁹ mixed photoresponsive molecules in a polydimethylsiloxane solution, and spun it to roughen the anodized aluminum surface. Water droplet adhesion on this modified surface became interchangeable by regulating the content of the functional molecules and using UV exposure. In the present study, our copolymer with adhesive functional groups assembled on a solid surface also exhibited a switchable wettability. On a flat titanium substrate modified with the present copolymer, after exposure to UV light (365 nm) for two hours, the contact angle decreases from ~90° to ~83°. And the original wettability also can be recovered after storing in dark. Several reversible cycles of contact angle were realized by UV radiation and storage in dark.

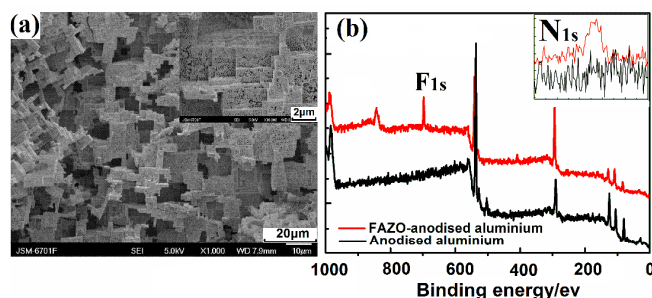


Fig. 4 (a) Low and high magnification SEM images of anodized aluminum; and (b) full XPS spectra and N fine spectra of modified and non-modified anodized aluminum.

In addition to assembling on nano-particle and flat surface, the copolymer also can modify on rough surface. The anodized aluminum sheet was prepared using an alternative anodization method³⁰. After anodization, innumerable micro steps and a series of nanowires appeared. The dual micro-nano structures lead to excellent superhydrophobic characteristics if modified using low-surface-energy materials³⁰. After modifying the adhesive and photoresponsive copolymer on the rough anodized aluminum sheet, a photoresponsive characteristic was achieved. The SEM images of the anodized aluminum sheet after modification with the polymer are shown in **Fig. 4a**. The random step structure was observed from the low magnification images, and a series of nanowires (about 100 nm) were observed on the step structures from the high magnification images. The full XPS spectra and N element fine spectra are shown in **Fig. 4b**. After the copolymer self-assembled on the anodized aluminum sheet, the F and N element singles proved that the copolymer successfully assembled.

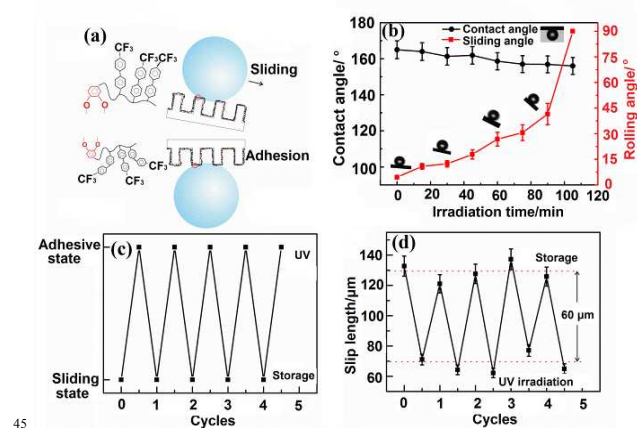


Fig 5 (a) Schematic map and corresponding digital image of adhesive state transformation; (b) variation of contact and sliding angles of modified rough sheet with increasing exposure time; (c) interchangeable cycles of adhesive state; and (d) slip length.

The wettability of the assembled surface is shown in **Fig. 5**. Before UV exposure, the -CF₃ group with low surface energy concentrated on the top surface because of the azobenzene with *trans* conformation, and excellent hydrophobic characteristics emerged. Moreover, a sliding state was also observed. After UV exposure for a certain time, the *trans* conformation of azobenzene molecules were gradually converted to the *cis* conformation. Some hydrogen bonds also formed between azobenzene groups and water molecules, and an adhesive state was achieved. After UV exposure and dark storage for a certain time, the sliding state recovered as the *cis* conformation slowly converted back to the *trans* conformation. **Fig. 5a** shows the schematic map and the contact angle images. Before UV exposure, the water droplet was able to slide down from the sheet surface with a slight tilt. After UV exposure, the water droplet adhered on the surface even as the sheets were overturned. With increasing exposure time, azobenzene molecules with *trans* conformation were transformed into the *cis* conformation gradually, which led to an increased surface adhesion. The sliding angle of the water droplet (**Fig. 5b**) was less than 5° without UV exposure, but with increasing exposure time, the sliding angles also increased and the water droplet adhered on the surface after UV exposure for 110 min. Moreover, the contact angles also slightly decreased. Because the extent of UV exposure is not enough, only a part of FAZO groups were transformed from *trans* to *cis* conformation. From the UV-vis absorption spectra of the copolymer (**Fig 1**), we found that about a half of FAZO groups have *trans-cis* conversion after UV exposure with 110 min. So, by controlling the UV exposure time, we can realize the change of surface adhesion but without wettability transformation.

When the liquids flow on a superhydrophobic surface, the slip length is usually used to describe the size of the boundary slippage. For planar Couette flow, the slip length b is defined as the distance inside the wall at which the extrapolated fluid velocity would equal the velocity of the wall³¹. From the definition, the slip length can written as :

$$b = \frac{v_s}{dv/dz}$$

where v_s is the slip velocity of the fluid on the surface, and dv/dz is the velocity gradient in the direction normal to the surface. Numerous methods that measure the slip length have already been reported. Examples of these methods are: fluorescent

recovery after photo-bleaching^{32, 33}, particle image velocimetry³⁴, which is based on tracing the fluid flow near a boundary; surface forces apparatus³⁵; atomic force microscopy³⁶, which is based on force or displacement; quartz crystal resonators³⁷; capillary techniques³⁸; and rheometer method^{39, 40}. For a superhydrophobic surface, measuring the rotation torque to determine the slip length is a feasible method. In this present study, we chose the rheometer method to measure the slip length. Here, plate-and-plate arrangement was applied to record the shear stress at a constant shear rate, and standard smooth stainless steel plate was used such that no-slip occurs when water flows on it. For systems with two parallel plates separated by a gap H , the slip length b of one of the two surfaces can be estimated as:

$$\frac{\tau_{\text{slip}}}{\tau_{\text{no-slip}}} = \frac{1}{1 + \frac{b}{H}}$$

where τ_{slip} and $\tau_{\text{no-slip}}$ are the shear stresses at the wall when slip and no-slip boundary conditions are applied, respectively. We measured the slip length on the responsive surface under different adhesive states (the adhesive and sliding state). Before UV exposure, the sliding angle was less than 5° , and there was a low adhesion force between the water droplet and the responsive surface. After UV exposure for a certain time, the water droplet adhered to the surface (high adhesion force) because of the *trans-cis* transformation of azobenzene. Moreover, after storage under dark conditions, the slippery state was recovered. The adhesive and slippery state can be interchanged by cycles of UV exposure and dark storage, as shown in Fig. 5c. The boundary slip is dependent on the adhesive state. Considering influence of the adhesive state, and excluding the edge effect of the water flow under the narrow gap of the rheometer⁴⁰, the contact angles of the two states were kept in a superhydrophobic state ($>150^\circ$). The slip length of slippery state was about 130 μm , and about 70 μm for the adhesive state (Fig. 5d). Similar to the adhesive state, the switching cycles of slip length be achieved by UV exposure and dark storage. Large differences in the slip length can be also regulated by UV exposure and dark storage. This responsive surface can be applied to intelligent fluid devices to achieve the fluid flow control.

Conclusions

A photoresponsive copolymer containing FAZO and DOPA was synthesized by free radical polymerization. The copolymer has a good film-forming property because of the DOPA groups. The copolymer was able to successfully self-assemble on TiO_2 nanoparticles, plane mica, and rough anodized aluminum surface. The copolymer also has a UV sensitive characteristic because of the FAZO group. When the copolymer assembled on the rough anodized aluminum sheet, the surface was endowed with superhydrophobic and photoresponsive characteristics. The surface adhesion can be regulated by UV exposure, and an interchangeable cycle between the adhesive and sliding state can be achieved using UV exposure and dark storage. The different adhesive states led to different surface slips on the responsive surface. The interchangeable slip length was measured using a rheometer. The surfaces that are capable of a considerable slippage effect have a wide potential for application in intelligent microfluidic devices and biodevices to help regulate the flow quantity in situ.

Acknowledgements

This work was financially supported by NSFC (21125316,

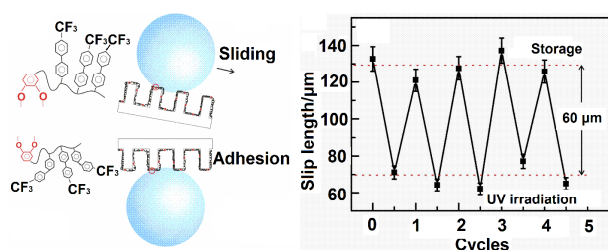
51305428, 51335010) and Key Research Program of CAS (KJZD-EW-M01).

Notes and references

- ^a State Key Laboratory of Solid Lubrication, Lanzhou Institute of Chemical Physics, Chinese Academy of Sciences, Lanzhou 730000, China
Corresponding author* Feng Zhou, zhouf@licp.cas.cn, 86-931-4968466.
^b University of Chinese Academy of Sciences, Beijing 100039, China
1. R. Blossey, *Nature Mater.*, 2003, **2**, 301.
 2. J. Wang, Q. Yang, M. Wang, C. Wang and L. Jiang, *Soft Matter*, 2012, **8**, 2261.
 3. T. Sun, L. Feng, X. Gao, L. Jiang, *Acc.Chem. Res.* 2005, **38**, 644.
 4. F. Xia and L. Jiang, *Adv. Mater.*, 2008, **20**, 2842.
 5. X. Zhang, F. Shi, J. Niu, Y. Jiang and Z. Wang, *J. Mater. Chem.*, 2007, **18**, 621.
 6. T. Chen, R. Ferris, J. Zhang, R. Ducker and S. Zauscher, *Prog Polym Sci*, 2010, **35**, 94.
 7. T. L. Sun, G. J. Wang, L. Feng, B. Q. Liu, Y. M. Ma, L. Jiang and D. B. Zhu, *Angew. Chem. Int. Edit.*, 2004, **43**, 357.
 8. H. S. Lim, J. T. Han, D. Kwak, M. Jin, and K. Cho, *J. Am. Chem. Soc.*, 2006, **128**, 14458.
 9. S. Minko, M. Muller, M. Motornov, M. Nitschke, K. Grundke, and M. Stamm, *J. Am. Chem. Soc.*, 2003, **125**, 3896.
 10. Z. Cheng, L. Feng and L. Jiang, *Adv. Funct. Mater.*, 2008, **18**, 3219.
 11. L. Xu, W. Chen, A. Mulchandani and Y. Yan, *Angew. Chem. Int. Edit.*, 2005, **44**, 6009.
 12. X. Liu, Q. Ye, B. Yu, Y. Liang, W. Liu, and F. Zhou, *Langmuir* 2010, **26**, 12377..
 13. D. Wang, Y. Liu, X. Liu, F. Zhou, W. Liu and Q. Xue, *Chem. Commun. (Camb)*, 2009, 7018..
 14. H. Lee, S. M. Dellatore, W. M. Miller and P. B. Messersmith, *Science*, 2007, **318**, 426..
 15. Q. Ye, F. Zhou and W. Liu, *Chem. Soc. Rev.*, 2011, **40**, 4244..
 16. S. M. Kang, N. S. Hwang, J. Yeom, S. Y. Park, P. B. Messersmith, I. S. Choi, R. Langer, D. G. Anderson and H. Lee, *Adv. Funct. Mater.*, 2012, **22**, 2949.
 17. X. W. Fan, L. J. Lin, J. L. Dalsin and P. B. Messersmith, *J. Am. Chem. Soc.*, 2005, **127**, 15843.
 18. K. Yang, J. S. Lee, J. Kim, Y. B. Lee, H. Shin, S. H. Um, J. B. Kim, K. I. Park, H. Lee and S. W. Cho, *Biomaterials*, 2012, **33**, 6952.
 19. A. Statz, J. Finlay, J. Dalsin, M. Callow, J. A. Callow and P. B. Messersmith, *Biofouling*, 2006, **22**, 391.
 20. B. H. Kim, D. H. Lee, J. Y. Kim, D. O. Shin, H. Y. Jeong, S. Hong, J. M. Yun, C. M. Koo, H. Lee and S. O. Kim, *Adv. Mater.*, 2011, **23**, 5618.
 21. S. M. Kang, I. You, W. K. Cho, H. K. Shon, T. G. Lee, I. S. Choi, J. M. Karp and H. Lee, *Angew. Chem. Int. Edit.*, 2010, **49**, 9401..
 22. H. Lee, Y. Lee, A. R. Statz, J. Rho, T. G. Park and P. B. Messersmith, *Adv. Mater.*, 2008, **20**, 1619..
 23. R. Truesdell, A. Mammoli, P. Vorobieff, F. van Swol and C. Brinker, *Phys.Rev.Lett.*, 2006, **97**, 044504.
 24. C. Lee and C.-J. C. Kim, *Langmuir*, 2009, **25**, 12812-12818.
 25. C. Lee, C.-H. Choi and C.-J. Kim, *Phys. Rev. Lett.*, 2008, **101**, 064501.
 26. Y. Wu, Y. Xue, X. Pei, M. Cai, H. Duan, W. T. S. Huck, F. Zhou and Q. Xue, *J. Phys. Chem. C*, 2014, **118**, 2564
 27. D. Prescher, T. Thiele, R. Ruhmann, G. Schulz *J. Fluorine Chem.*, 1995, **74**, 185.
 28. X. Wang, Q. Ye, J. Liu, X. Liu and F. Zhou, *J. Colloid Interface Sci.*, 2010, **351**, 261.
 29. X. Liu, M. Cai, Y. Liang, F. Zhou and W. Liu, *Soft Matter*, 2011, **7**, 3331.
 30. W. Wu, X. Wang, D. Wang, M. Chen, F. Zhou, W. Liu and Q. Xue, *Chem Commun (Camb)*, 2009, 1043.
 31. R. S. Voronov, D. V. Papavassiliou, *Ind. Eng. Chem. Res.*, 2008, **47**, 2455.

32. R. Pit, H. Hervet, L. Léger, *Tribol. Lett.*, 1999, **7**, 147.
 33. H. Hervet and L. Léger, *Comptes Rendus Physique*, 2003, **4**, 241.
 34. P. Joseph and P. Tabeling, *Phys. Rev. E*, 2005, **71**, 035303.
 5 35. Y. Zhu and S. Granick, *Phys. Rev. Lett.*, 2001, **87**, 096105.
 36. C. L. Henry, C. Neto, D. R. Evans, S. Biggs and V. S. J. Craig, *Physica A: Statistical Mechanics and its Applications*, 2004, **339**, 60.
 37. B. Du, I. Goubaidoulline and D. Johannsmann, *Langmuir*, 2004, **20**, 10617.
 10 38. C.-H. Choi, U. Ulmanella, J. Kim, C.-M. Ho and C.-J. Kim, *Phys. Fluids*, 2006, **18**, 087105.
 39. M. Zhou, J. Li, C. Wu, X. Zhou and L. Cai, *Soft Matter*, 2011, **7**, 4391.
 15 40. C.-H. Choi and C.-J. Kim, *Phys. Rev. Lett.*, 2006, **96**, 066001.

20 A table of contents entry



A photo-switchable boundary slippage was realized by means of modification with UV-sensitive copolymer on rough anodised aluminium.
 25